EARTHQUAKE ENGINEERING AND STRUCTURAL DYNAMICS, VOL. 26, 1157–1167 (1997)

SYSTEM IDENTIFICATION OF THE HUALIEN LSST MODEL STRUCTURE

TOSHIO KOBAYASHI,[1]* SATOSHI KAN,[1] HIROYOSHI YAMAYA[1] AND EIJI KITAMURA[2]

[1]*Kajima Technical Research Institute, Chofu-shi, Tokyo 182, Japan*
[2]*Kajima Information Processing Center, Kajima Corporation, Minato-ku, Tokyo 107, Japan*

SUMMARY

This paper discusses system identification of a $\frac{1}{4}$-scale nuclear reactor containment Soil–Structure Interaction system (SSI system) based on forced vibration tests conducted by an exciter. For both NS and EW excitations, response components orthogonal to the exciting directions were fairly large because of inhomogeneity of the supporting soil, so, before applying the system identification procedure, the concept of 'Principal Axes (D_1, D_2)' was introduced for the SSI system. The tests results were then transposed to the principal axis directions so that the orthogonal components disappeared.[1] The system identification procedure was applied to these principal axis directions. As a result, fundamental frequency, damping factor and mode shape with fixed-base condition were obtained. A mathematical model was thus established by adjusting the calculated fundamental frequency and mode shape with fixed-base condition to these derived from the test results. The mathematical model will be used in the correlation analysis of both forced vibration tests and earthquake observation records. © 1997 John Wiley & Sons, Ltd.

Earthquake Engng. Struct. Dyn., **26**, 1157–1167 (1997)

No. of Figures: 15. No. of Tables: 2. No. of References: 8.

KEY WORDS: soil–structure interaction; nuclear power plant; forced vibration test; system identification; soil inhomogeneity; principal axis

1. INTRODUCTION

A Large-Scale Seismic Test (LSST) Program[2] was conducted at Hualien (stiff-soil site), Taiwan, to obtain earthquake-induced Soil–Structure Interaction (SSI) data. This program was undertaken as an extension to the same kind of program conducted at Lotung (soft-soil site). Before starting earthquake observations, forced vibration tests using an exciter were conducted to obtain basic dynamic characteristics of the soil–structure interaction system. Two tests were performed: (1) a Forced Vibration Test without embedment (FVT-1)[3] and (2) the same test with embedment (FVT-2).[4] This paper discusses system identification of the model structure. Although the method of identification applied here is not original, it is invaluable to discuss the process from forced vibration test data to identified result which confirm the applicability of the theory to real large-scale structure. A photograph and a section of the model structure are shown in Figures 1 and 2, respectively.

2. TEST RESULTS

As to the excitation direction, horizontal NS and EW and vertical tests were performed for the first-floor excitation and horizontal NS and EW tests were performed for the roof-floor excitation, for both FVT-1 and FVT-2. This paper discusses only the horizontal directions.

* Correspondence to: Toshio Kobayashi, Kajima Technical Research Institute, Chofu-shi, Tokyo 182, Japan

Contract grant sponsor: Tokyo Electric Power Company

CCC 0098–8847/97/111157–11$17·50

Received 27 January 1997
Revised 25 April 1997

Figure 1. Photograph of the model structure

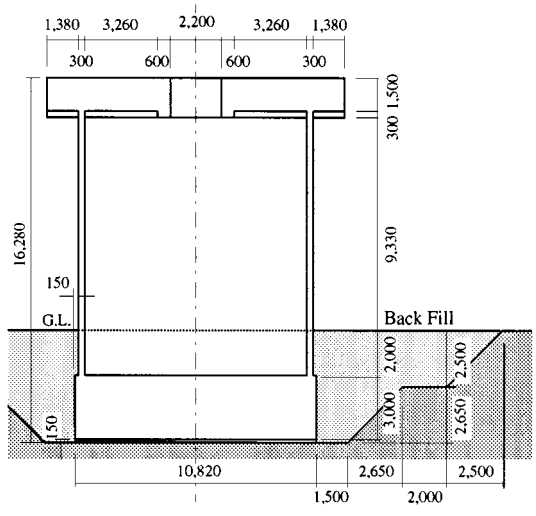

Figure 2. Section of the model structure

As for exciting force level, in addition to main excitation level, the responses for $\frac{1}{3}$ and 3 times of main excitation level were compared around peak frequency and the differences were negligible small. It concluded that the response for main excitation level remained in linear range.

Figures 3 and 4 show the horizontal displacement resonance curves of FVT-1 for NS and EW and principal axis (D_1, D_2) direction excitations at the roof, respectively. In Figure 3, the resonance curves have two peaks: at 4·1 and 4·6 Hz. The components orthogonal to the exciting directions are about 60 per cent of those in the exciting direction. Figure 4 shows the result of transposing Figure 3 to the principal axis directions, D1 and D2. The resonance curves have single peaks at 4·1 and 4·6 Hz, respectively. The components orthogonal to the exciting directions are negligible. Figures 5 and 6 are similar to Figures 3 and 4, but are FVT-2. Figure 5 shows resonance curves for NS and EW excitations, where the components orthogonal to the exciting directions are about 20 per cent of those in the exciting directions. Figure 6 shows

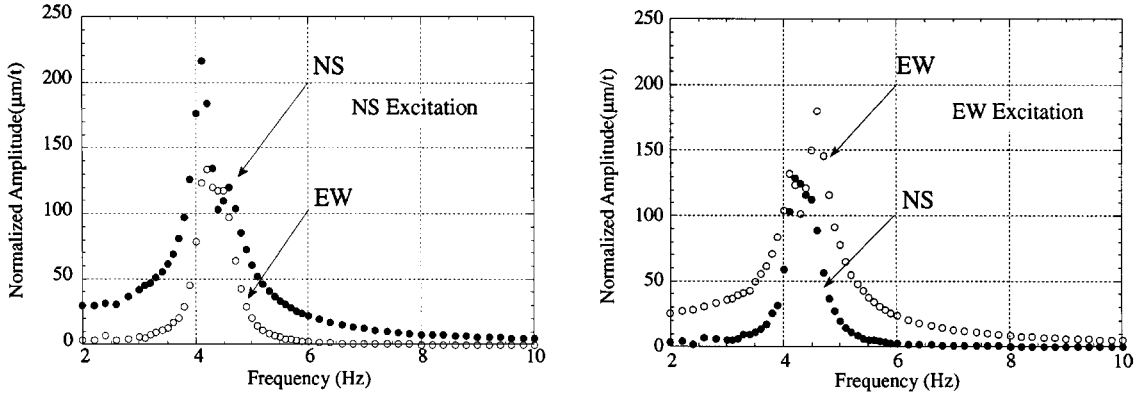

Figure 3. Resonance curves at roof for NS and EW excitation without backfill

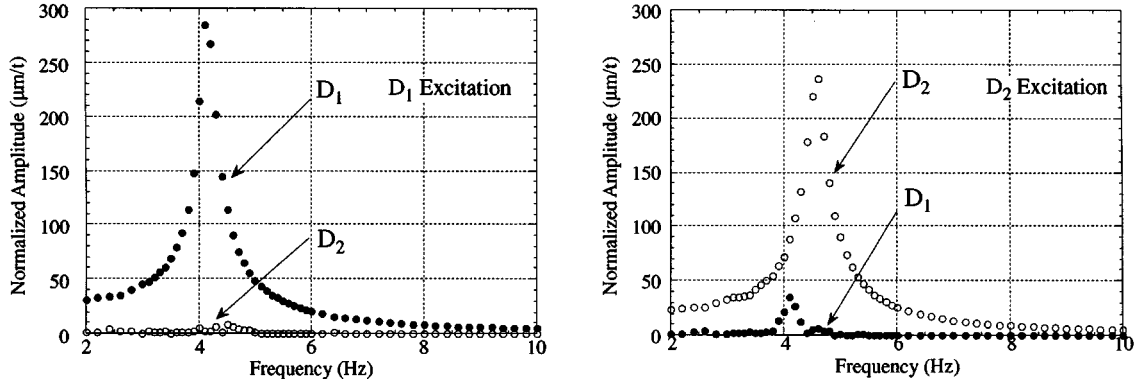

Figure 4. Resonance curves at roof for D_1 and D_2 excitation without backfill

resonance curves for principal axis excitation, in which the orthogonal components are also negligible. This means that the responses for NS and EW excitations are coupled to each other and exciting energies are separated to each direction. The responses for D1 and D2 excitations are not coupled to each other and exciting energy is concentrated to the exciting direction. The angles of the principal axis counterclockwise from plant north direction are obtained as 34° without embedment and 30° with embedment by an eigenvalue analysis for a variance–covariance matrix.[4]

The reason why the dynamic characteristics of this cylindrical soil-structure system are not axi-symmetric was considered to be the inhomogeneity of the supporting soil[4] and this was confirmed by the simulation analysis.[5]

The test results of the NS and EW excitations are complicated (two-peak resonance curve or orthogonal component responses) because of the coupling effect, but they are simplified by transposing them to the principal axis direction in which the responses are decoupled. Based on these transposed results, peak frequencies, damping factors and displacement component ratios (sway, rocking and elastic deformation of the structure) at the roof floor in the fundamental mode shapes are obtained as shown in Table I. The system identification procedure is applied for these transposed results to the principal axis directions.

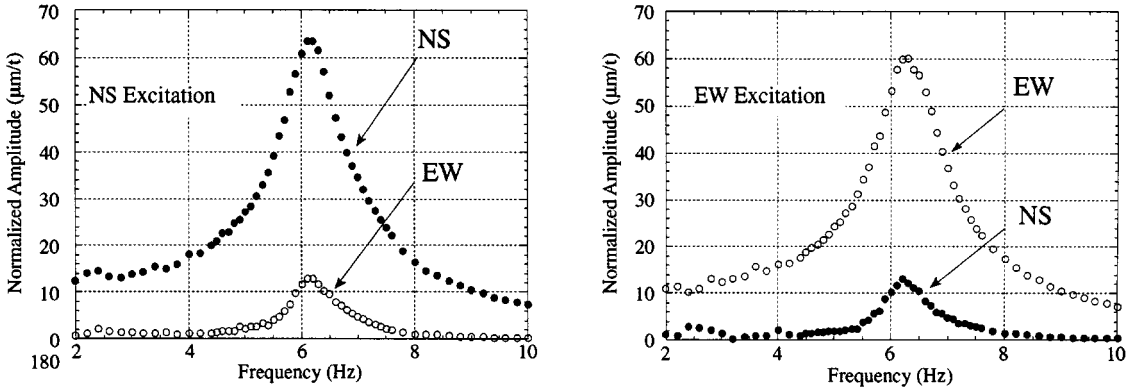

Figure 5. Resonance curves at roof for NS and EW excitation with backfill

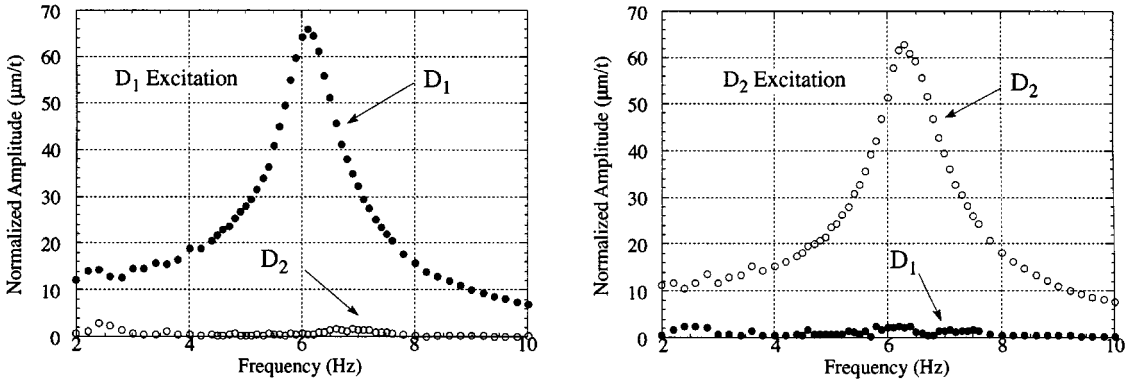

Figure 6. Resonance curves at roof for D_1 and D_2 excitation with backfill

Table I. Test results for horizontal excitation at first floor

Direction	Peak frequency (Hz)	Damping factor (%)	Deformation ratio (%)		
			Sway	Rocking	Elastic deformation
FVT-1(D1)	4·2	3·6	14	61	25
FVT-1(D2)	4·6	3·7	12	66	22
FVT-2(D1)	6·5	8·6	5	55	40
FVT-2(D2)	6·6	8·1	6	48	46

3. DYNAMIC CHARACTERISTICS OF MODEL STRUCTURE

3.1. Dynamic characteristics with fixed-base condition

The dynamic characteristics of the model structure under the fixed-base condition were derived from forced-vibration test results by a system identification method.[6] These results yielded pure structural dynamic characteristics that exclude soil–structure interaction effects.

For the first-floor excitation, the dynamic equation system of motion with sway (z), rocking (θ) and elastic deformation of superstructure above basemat (x) is given in matrix form as equation (1) and the elastic deformation vector (x) is expressed by equation (2).

$$M(\ddot{x} + I\ddot{z} + H\ddot{\theta}) + C\dot{x} + Kx = 0 \tag{1}$$

$$x = \sum_{j=1}^{N} X_j q_j \tag{2}$$

where M, C and K are mass, damping and stiffness matrices of the superstructure, and I and H are unit and height vector, respectively. X_j is the jth mode vector and q_j is the jth time function. Multiplying by the transposed first-mode vector from the left side and considering the orthogonal condition between different mode vectors, the dynamic equation of motion of the first mode is given by

$$X_1^{\mathrm{T}} M X_1 \ddot{q}_1 + X_1^{\mathrm{T}} M I \ddot{z} + X_1^{\mathrm{T}} M H \ddot{\theta} + X_1^{\mathrm{T}} C X_1 \dot{q}_1 + X_1^{\mathrm{T}} K X_1 q_1 = 0 \tag{3}$$

The following expressions are then introduced for simplicity:

$$\bar{\omega}^2 = \frac{X_1^{\mathrm{T}} K X_1}{X_1^{\mathrm{T}} M X_1} \quad 2h\bar{\omega} = \frac{X_1^{\mathrm{T}} C X_1}{X_1^{\mathrm{T}} M X_1} \quad \alpha = \frac{X_1^{\mathrm{T}} M I}{X_1^{\mathrm{T}} M X_1} \quad \gamma = \frac{X_1^{\mathrm{T}} M H}{X_1^{\mathrm{T}} M X_1} \tag{4}$$

Furthermore, sinusoidal time functions are expressed as

$$q_1 = Q\mathrm{e}^{\mathrm{i}\omega t} \quad z = Z\mathrm{e}^{\mathrm{i}\omega t} \quad \theta = \Theta\mathrm{e}^{\mathrm{i}\omega t} \tag{5}$$

Applying these expressions to equation (3), the first-mode response of the elastic deformation component for sway and rocking input motion can be derived as

$$Q = \frac{\omega^2(\alpha Z + \gamma\Theta)}{\bar{\omega}^2 - \omega^2 + 2\mathrm{i}h\omega\bar{\omega}} \tag{6}$$

The dynamic equation of motion with only elastic deformation (fixed-base condition) for sway input acceleration ($\ddot{z}_0$) is given by equation (7) and the elastic deformation vector $\bar{x}$ is given by equation (8).

$$M(\ddot{\bar{x}} + I\ddot{z}_0) + C\dot{\bar{x}} + K\bar{x} = 0 \tag{7}$$

$$\bar{x} = \sum_{j=1}^{N} X_j \bar{q}_j \tag{8}$$

where $\bar{q}_j$ is the jth time function. Multiplying by the transposed first-mode vector from the left side, and considering the orthogonal condition between different mode vectors, the dynamic equation of motion of the first mode is given by

$$X_1^{\mathrm{T}} M X_1 \ddot{\bar{q}}_1 + X_1^{\mathrm{T}} M I \ddot{z}_0 + X_1^{\mathrm{T}} C X_1 \dot{\bar{q}}_1 + X_1^{T} K X_1 \bar{q}_1 = 0 \tag{9}$$

Here again, sinusoidal time functions are expressed as

$$\bar{q}_1 = \bar{Q}\mathrm{e}^{\mathrm{i}\omega t} \quad \ddot{z}_0 = \ddot{Z}_0\,\mathrm{e}^{\mathrm{i}\omega t} \tag{10}$$

By applying equations (4), (5) and (10) to equation (9), it is concluded that the first-mode response of the elastic deformation component of the dynamic system with only elastic deformation (fixed-base condition) for unit base sway acceleration input ($\ddot{Z}_0 = 1$) is given by

$$\bar{Q} = \frac{-\alpha\ddot{Z}_0}{\bar{\omega}^2 - \omega^2 + 2\mathrm{i}h\omega\bar{\omega}} \quad \text{where} \quad \ddot{Z}_0 = 1 \tag{11}$$

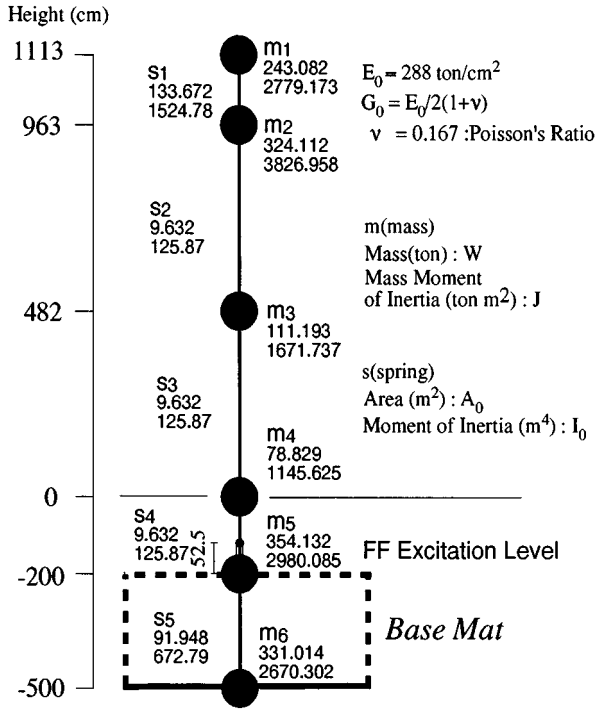

Figure 7. Lumped mass model

Comparing equations (6) and (11), the first-mode response of the elastic deformation component ($\bar{Q}$) with fixed-base condition for unit base sway acceleration input is given by the first-mode response of the elastic deformation component (Q) of the dynamic system with sway, rocking and elastic deformation as

$$\bar{Q} = Q \times \frac{-\alpha \ddot{Z}_0}{\omega^2(\alpha Z + \gamma \Theta)} = Q \times \frac{-\alpha}{\omega^2(\alpha Z + \gamma \Theta)} \tag{12}$$

3.2. Mathematical model of structure

The mass matrix and the height vector of the model structure are evaluated from design drawing geometry as shown in Figure 7. The mode shape for the elastic deformation component is represented by the ratio of rotational angle (θ) to horizontal displacement (u) at the roof floor (RF), which are produced by elastic deformation of the superstructure above basemat. The observed mode ratio (θ/u) derived from FVT-2 results is shown in Figure 8. It is nearly equal to $5{\cdot}5 \times 10^{-4}$ rad/cm except in the frequency range below 5 Hz, which is used to evaluate the first-mode vector of elastic deformation (X_1).

The reason of scattering of plots for frequency range below 5 Hz in Figure 8 is considered to be ill condition of signal/noise ratio by following facts:

(1) (u) is contaminated by noise easily compared to measured response itself because (u) is derived from roof horizontal response subtracting base horizontal response and rocking response component.
(2) An eccentric mass-type exciter was used for the tests and its exciting force was proportional to the square of exciting frequency. The exciting force below 5 Hz was not large enough to derive (u) compared to noise.

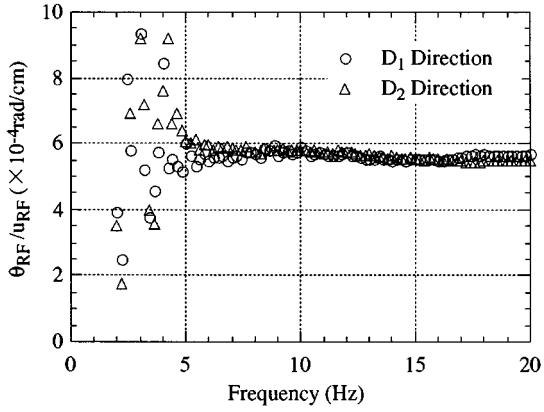

Figure 8. Observed mode ratio (θ/u) derived from FVT-2 test results

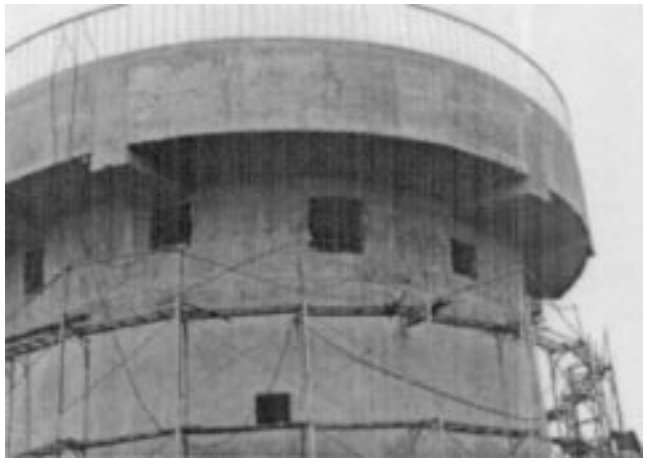

Figure 9. Large holes at shell wall top

In addition to the same reason, FVT-1 results could not be used for derivation of mode ratio (θ/u) because FVT-1 should start only one week after the concrete casting to ten large-holes at shell wall top (See Figure 9). The dynamic characteristics of the model structure were considered to change slightly during FVT-1 which continued two weeks. This change affected little on measured response itself but it affected seriously on the derived mode ratio (θ/u) by the reason mentioned above and the results are not stable as shown in Figure 10.

Considering these conditions, a stable value ($5{\cdot}5 \times 10^{-4}$ rad/cm) derived from FVT-2 results is applied for a mode ratio (θ/u) both for FVT-1 and FVT-2 analyses.

These data are used to obtain values of α and γ defined by equation (4). From equation (12), resonance curves for fixed-base condition ($\bar{Q}$) are obtained by applying measured sway (Z) and rocking (Θ) of the base and elastic deformation resonance curves (Q). The resonance curves for the fixed-base condition derived from the test results are shown in Figures 11–14, in which the regression results to the one-degree-of-freedom resonance curves are also shown.

Natural frequencies and damping factors obtained by the regression method are summarized in Table II. The averaged values of natural frequency and damping factor are 9·54 Hz and 1·0 per cent respectively.

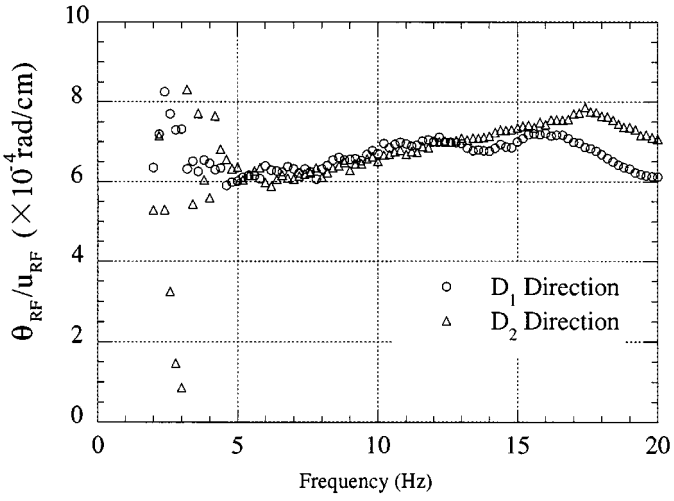

Figure 10. Observed mode ratio (θ/u) derived from FVT-1 test results

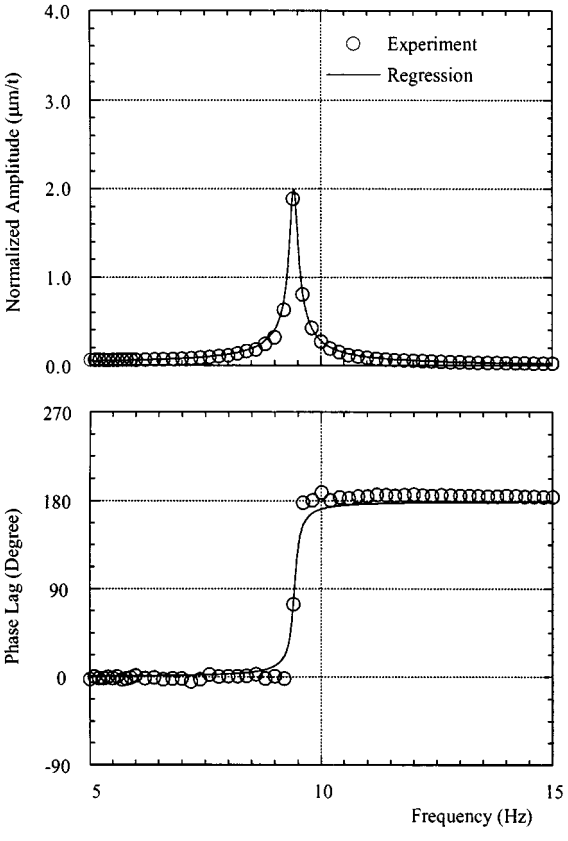

Figure 11. Resonance curves for fixed-base condition (FVT-1, D_1 direction)

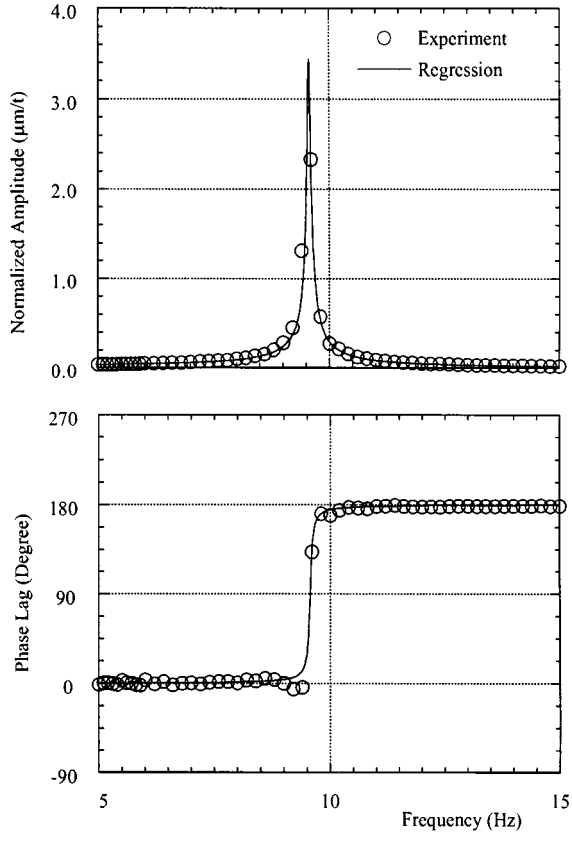

Figure 12. Resonance curves for fixed-base condition (FVT-1, D_2 direction)

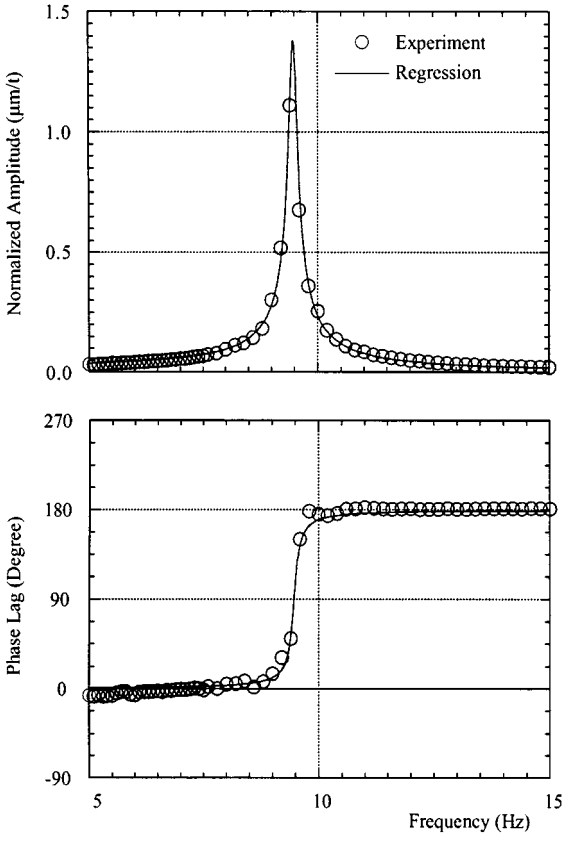

Figure 13. Resonance curves for fixed-base condition (FVT-2, D_1 direction)

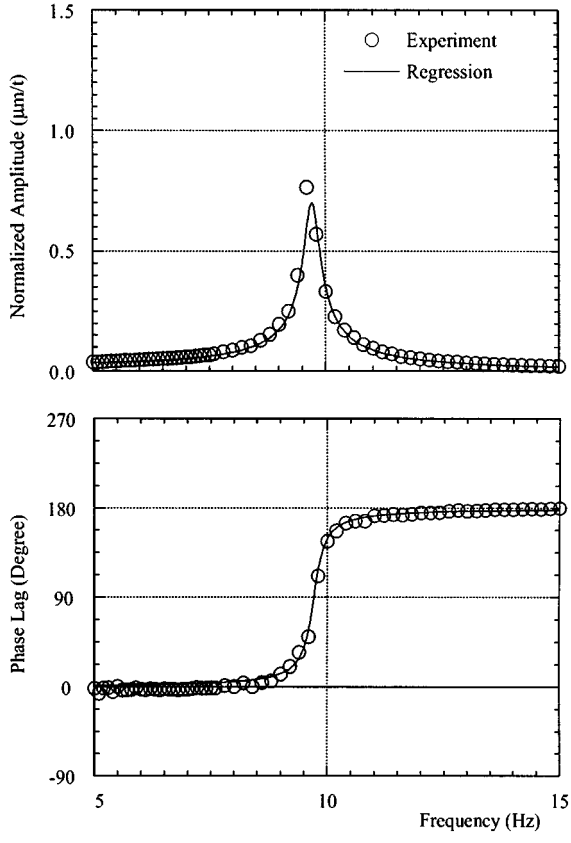

Figure 14. Resonance curves for fixed-base condition (FVT-2, D_2 direction)

Table II. Regression results

Direction	Test results				Fixed-base condition			
	FVT-1		FVT-2		FVT-1		FVT-2	
	f_0 (Hz)	h (%)	f_0 (Hz)	h (%)	f_{f0} (Hz)	h_f (%)	f_{f0} (Hz)	h_f (%)
D1	4·2	3·6	6·5	8·6	9·42	0·9	9·47	1·0
D2	4·6	3·7	6·6	8·1	9·56	0·4	9·71	1·8

Note: f_0: peak frequency, h: damping factor, average: $f_{f0} = 9{\cdot}54$ Hz, $h_f = 1{\cdot}0\%$

Mode ratio (θ/u) calculated from the flexural and shear beam model is shown in Figure 15, in which the geometrical coefficient for shear deformation (κ) is considered as a parameter. A mode ratio of $5{\cdot}5 \times 10^{-4}$ rad/cm is derived from this figure, when the geometrical coefficient for shear deformation (κ) is roughly equal to 0·5.

Calculated fundamental frequency for the fixed-base condition is also shown in Figure 15, in which Young's modulus is considered to be $E_0 = 288$ ton/cm^2 which was derived from the cylinder test results, and

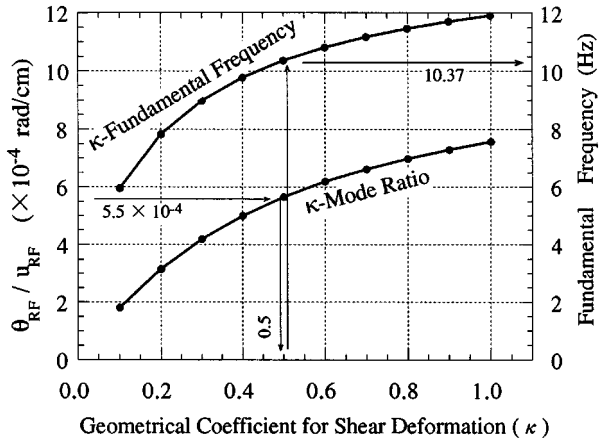

Figure 15. Relations between geometrical coefficient for shear deformation and mode ratio (θ/u), fundamental frequency

the geometrical coefficient for shear deformation (κ) is considered as a parameter. From this figure, the fundamental frequency is 10·37 Hz when the geometrical coefficient for shear deformation (κ) is equal to 0·5.

To adjust the calculated fundamental frequency (10·37 Hz) to that derived from the test results (averaged to 9·54 Hz) as aforementioned, Young's modulus is revised to effective Young's modulus (E_e) using an apparent stiffness reduction factor (η) as follows:

$$E_e = \eta \times E_0 = 0{\cdot}85 \times 288 \text{ ton/cm}^2 = 243 \text{ ton/cm}^2$$

$$\eta = (9{\cdot}54 \text{ Hz}/10{\cdot}37 \text{ Hz})^2 = 0{\cdot}85$$

The reasons for the apparent stiffness reduction effect are considered to be as follows:

(1) Geometry of the model structure as built is different from that of the design drawings.
(2) Stress transfer mechanism is different from that of an idealized cylindrical wall because of the complicated construction process (there were large openings on the cylindrical wall that were infilled before completion).
(3) There is a possibility that the concrete material properties of the structure are different from those of the test specimen.

However, it is difficult to discuss quantitative participation values of these effects on η.

4. CONCLUSIONS

Concluding remarks obtained from the analysis results are summarized as follows:

(1) Fundamental frequency and damping factor of the model structure with fixed-base condition are obtained from the forced vibration test results by the system identification method to be 9·54 Hz and 1·0 per cent respectively.
(2) The structural mathematical dynamic models were established. The geometrical coefficient for shear deformation (κ) and effective Young's modulus are equal to 0·5 and 243 ton/cm^2, respectively.

ACKNOWLEDGEMENTS

The research reported here-in was conducted as one part of subcontract on Hualien Project from Tokyo Electric Power Company to Kajima Technical Research Institute. The authors wish to express their gratitude for Tokyo Electric Power Company for giving the permission to publish this work.

REFERENCES

1. H. Yamaya, T. Kobayashi and T. Sugiyama, 'Study on forced vibration tests for large scale SSI model' (in Japanese), *J. Struct. Construction Engng.* (*Trans. of AIJ*), **478**, 81–90 (1995).
2. H. T. Tang *et al.*, 'The Hualien large-scale seismic test for soil–structure interaction research', *Proc. 11th SMiRT: K04/4.* Tokyo, Japan, 1991.
3. H. Morishita, H. Tanaka, N. Nakamura, T. Kobayashi, S. Kan, H. Yamaya and H. T. Tang, 'Forced vibration test of the Hualien large scale SSI model', *Proc. 12th SMiRT: K02/1*, Stuttgart, Germany, 1993.
4. Y. Sugawara, T. Uetake, T. Kobayashi and H. Yamaya, 'Forced vibration test of the Hualien large scale SSI model (Part 2)', *Proc. 13th SMiRT: KA05/1*, Port Algere, Brazil, 1995, pp. 109–114.
5. K. Yoshida, 'Fundamental studies on soil–structure interaction problems', *Doctorial Thesis*, Tohoku University, 1995.
6. T. Ishibashi and Y. Naito, 'System identification methods of buildings considering rocking motion of the base', *Annual Report, KAJIMA Technical Research Institute*, Vol. 42 (1994).
7. T. Kobayashi, M. Nakazawa, T. Sugiyama and H. Yamaya, 'Forced vibration test of Hualien large-scale soil–structure interaction model (Part 7) Dynamic characteristics of fixed base model', *Summaries of Technical Papers of Annual Meeting, Architectural Institute of Japan*, 1995, Paper No. 21549.
8. T. Kobayashi, H. Yamaya, E. Kitamura and T. Sugiyama, 'System identification of the Hualien LSST model structure', *Proc. 11th World Conf. on Earthquake Engineering, Paper No. 67,* Acapulco, Mexico, 1996.

